Available online at www.sciencedirect.com
SCIENCE DIRECT®
Journal of Sound and Vibration 275 (2004) 107–126
JOURNAL OF SOUND AND VIBRATION
www.elsevier.com/locate/jsvi

Cyclic modulation of semi-active controllable dampers for tonal vibration isolation

P. Anusonti-Inthra, F. Gandhi*

Department of Aerospace Engineering, The Pennsylvania State University, 229 Hammond Building, University Park, PA 16802, USA

Received 10 January 2002; accepted 18 June 2003

Abstract

The present study examines the potential of using a semi-active controllable damper, whose damping coefficient can be modulated in real time, for tonal vibration isolation applications. A frequency-domain control algorithm is developed for determining the damping coefficient variation (at twice the disturbance frequency) that minimizes the force transmitted to the support at the disturbance frequency. The effectiveness of open-loop, closed-loop, and adaptive controllers in rejecting the transmitted disturbances are evaluated. The results of the study indicate that when limits in damping coefficient variation are considered, the support force could be reduced by about an additional 30%, beyond the levels due to the passive isolation characteristics (no cyclic damping modulation). When the disturbance phase changes during operation, the effectiveness of the open-loop controller is rapidly degraded. While the closed-loop controller (with inputs based on current levels of force transmitted to the support) performed better, there was still some degradation in performance, and transmitted support forces were not reduced to levels prior to the change in disturbance phase. The results show that for the semi-active system to retain its effectiveness in rejecting disturbances, a closed-loop, adaptive controller (with on-line system identification) is required; even when there is only a change in disturbance, and no change in basic system properties. An explanation for this phenomenon, related to the bi-linear nature of the semi-active system, is provided. Cyclic modulations in the damping coefficient were more effective in reducing the transmitted forces at the disturbance frequency than simply reducing the baseline damping coefficient (to improve the passive isolation characteristics).

*Corresponding author. Tel.: +1-814-865-1164; fax: +1-814-8654-7092.
E-mail address: fgandhi@psu.edu (F. Gandhi).

0022-460X/$ - see front matter © 2003 Elsevier Ltd. All rights reserved.
doi:10.1016/S0022-460X(03)00788-0

1. Introduction

Undesirable vibrations in many engineering applications are often concentrated in a narrow frequency range. Such narrowband vibrations could, for example, be produced by rotating machinery—electric motors, fans and propellers, helicopter rotors, etc. Without any treatment, the vibrations of the system, as well as the vibration energy transmitted to the support, could potentially compromise performance and reduce component life. In the case of helicopter rotors and propeller-driven aircraft, the vibration energy transmitted to the fuselage results in human fatigue and reduced ride comfort, as well. Thus, considerable effort has been devoted in the past to suppress and isolate narrowband vibrations, using both passive design concepts as well as active strategies (see, for example, Refs. [1–11]).

Common passive techniques for reduction of narrowband vibrations, or rejection of tonal disturbances, include the use of vibration absorbers and isolation schemes. While these concepts can be reasonably successful, there is usually a weight penalty involved, and their effectiveness can be significantly reduced with changes in operating conditions (for example, frequency of the disturbance) as well as changes in properties of the system. Active vibration suppression strategies such as active mounts, active truss modules, and active control of structural response (ACSR—used in helicopters) employ actuators to provide active forces for directly canceling the vibratory forces. Although active methods can be very effective and can be configured to cope with a change in incoming disturbances (through closed-loop controllers) and variation in system properties (through adaptive controllers), they usually require significant power and actuator authority.

In recent years, a new approach, known as *semi-active control*, has been receiving increasing attention for vibration reduction applications. In this approach, system properties such as damping or stiffness are controlled to modify the system response and reduce vibration. Since large active forces are not being directly applied to the system (as in the case of active vibration reduction schemes), semi-active control schemes are characterized by very low-power requirements, while still retaining the ability to adapt to changes in conditions. Additionally, with semi-active approaches the risk for instability is practically eliminated, because unlike active approaches, energy is not being pumped into the controlled system. The majority of the studies on semi-active concepts are focused on *broadband* vibration suppression and isolation applications such as controlling seismic response (see, for example, Refs. [12–15]) and in the design of suspensions in the automobile industry (see, for example, Refs. [16–19]). In recent years, there has also been a strong interest in the use of semi-active controllable dampers for helicopter applications (see, for example, Refs. [20–23]). Controllable rotor blade lag dampers can be exploited to provide high levels of damping in critical operating conditions while reducing the damping levels during non-critical flight conditions so as to reduce damper and blade periodic loads and increase component fatigue life. In addition, there is the possibility of modulating the damping levels over every rotor revolution, at harmonics of the rotational speed, to reduce the rotor hub vibrations [23]. For practical implementation of the semi-active control concept, a wide range of discrete devices are available that can change the effective damping or stiffness characteristics of the system into which they are introduced. These include stiffness control devices, electrorheological and magnetorheological dampers, friction control devices, controllable orifice devices, and tuned mass/liquid dampers (see Ref. [24] for a detailed description of such devices).

Although vibration reduction using semi-active concepts are attractive for the reasons cited above, special control algorithms have to be developed, since the semi-active system is non-linear, or specifically bi-linear, in nature. One of the most commonly used algorithms is based on the LQR clipped-optimal control scheme [14,25–29]. Other algorithms include "bang–bang" or "on–off" controllers (see, for example, Refs. [15,29–31]), controllers with a more sophisticated scheduled input [32], and fuzzy-logic controllers [33]. Some researchers have also used non-linear sliding-mode controllers [12,27]. All of the above studies have clearly demonstrated that semi-active control systems are quite effective in reducing broadband vibrations, but so far, there has been little effort to exploit semi-active control for narrowband disturbance rejection.

2. Focus of the present study

The primary focus of the present study is to examine the potential of using semi-active control for narrowband disturbance rejection applications (the tonal vibration isolation problem). The system considered uses a semi-active controllable damper whose effective damping coefficient can be modulated in real time. For a harmonic disturbance, a frequency-domain control algorithm is developed that determines the controllable damper inputs (cyclic variation in damping coefficient) for minimizing the forces transmitted to the support. The effectiveness of open-loop, closed-loop, and adaptive controllers in rejecting the transmitted disturbances are evaluated.

3. Analysis

3.1. System description

To evaluate the effectiveness of the semi-active controllable damper for rejecting narrowband disturbances (tonal vibration isolation), a simple single-degree-of-freedom (SDOF) system is considered, as shown in Fig. 1. The mass, m, supported on the semi-active controllable damper

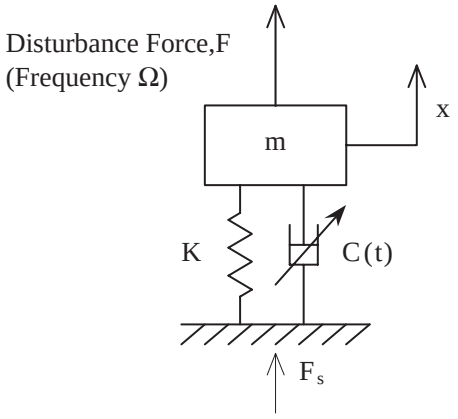

Fig. 1. Schematic of single-degree-of-freedom system with controllable damper (representing a semi-active isolation system).

and parallel spring, is subjected to a harmonic disturbance force of amplitude, F_0, and frequency, Ω. The total damping coefficient of the semi-active damper is expressed as

$$C(t) = C_0 + C_1 u(t), \tag{1}$$

where C_0 represents the baseline (passive) damping, and $C_1 u(t)$ represents the variation in damping due to the command input u (following the approach cited in Ref. [27]). Rejection of the incoming disturbance (at frequency Ω) is achieved by cyclically modulating the damping coefficient of the semi-active controllable damper. Without any modulation of the damping coefficient ($u = 0$), the spring, K, in parallel with the baseline damper, C_0, provides a passive isolation treatment between the disturbance force, F_0, and the force transmitted to the support, F_s.

The equilibrium equation for the system in Fig. 1, and the corresponding force at the support, can be expressed as

$$m\ddot{x} + (C_0 + C_1 u)\dot{x} + Kx = F = F_0 \sin(\Omega t), \quad F_s = (C_0 + C_1 u)\dot{x} + Kx. \tag{2a, b}$$

The bilinear term, $u\dot{x}$, which appears in the above equations (such a bilinear term appears in most semi-active systems), makes it difficult to apply conventional linear control theories.

3.2. Fundamentals of controller design

3.2.1. Overview of the semi-active controller for narrowband disturbance rejection

For narrowband disturbance rejection using a semi-active controllable damper, a frequency-domain controller is developed, as an adaptation of the approach presented in Ref. [34] for disturbance rejection using pure active control. The vibratory force transmitted to the support, F_s, and the command input, u, are expressed in the frequency domain (as cosine and sine components at specified harmonics of the fundamental frequency, Ω), and are denoted as z and u_c, respectively. To reject the incoming disturbance at frequency Ω transmitted to the support, a second harmonic (2Ω) input, u_c, is primarily required (see Section 3.2.3 for detail); although additional harmonics could be included as well in certain cases. The control algorithm is based on the minimization of a quadratic objective function, J, defined as

$$J = z^{\mathrm{T}} W_1 z + u_c^{\mathrm{T}} W_2 u_c. \tag{3}$$

In the above equation, W_1 and W_2 represent penalty weighting corresponding to the vibratory force at the support, z, and the input, u_c, respectively.

Due to the bilinear term in Eqs. (2), the relationship between the input, u_c, and the support vibration, z, is not linear. However, the sensitivity of the vibratory forces transmitted to the support, z, to perturbations in the frequency-domain inputs, u_c, are still expressed as

$$z = z_0 + T u_c, \tag{4}$$

where T is the system transfer matrix, and z_0 represents the baseline support vibration levels without the input, u_c. The transfer matrix, T, can be calculated using both off-line and on-line approaches (detail discussion is presented in Section 3.2.4). A gradient-based method is used to minimize J and determine the inputs, u_c. By substituting Eq. (4) into Eq. (3) and setting $\partial J/\partial u_c = 0$, the resulting input may be obtained as

$$u_c = \bar{T} z_0, \quad \bar{T} = -(T^{\mathrm{T}} W_1 T + W_2)^{-1} T^{\mathrm{T}} W_1. \tag{5a, b}$$

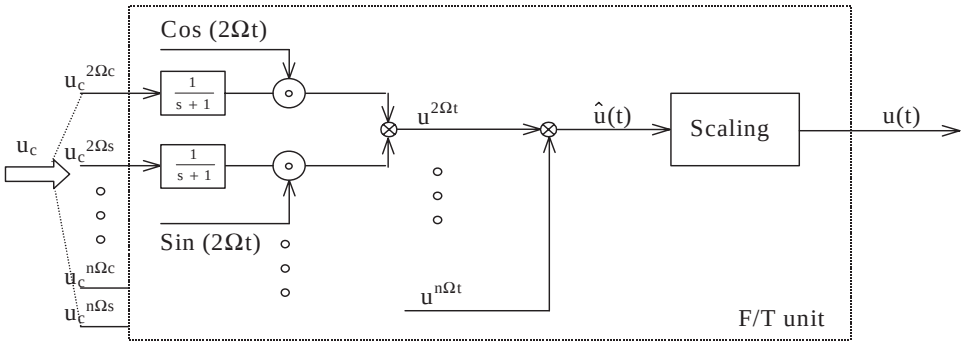

Fig. 2. Frequency-to-time domain conversion (F/T) unit.

It should be noted that if the system was linear (the bi-linear nature of the system in Eq. (2) is entirely due to the semi-active control introduced, and would be absent if pure active control was used), Eq. (4) would be rigorously valid, and the inputs calculated in Eq. (5) would then be optimal inputs (this would essentially be an implementation of the optimal control algorithm in the frequency domain [34]). For the semi-active bi-linear system, Eq. (4) is an approximation, and the inputs calculated in Eq. (5) could therefore be sub-optimal. It should also be noted that although a disturbance amplitude, F_0, is specified for the simulations in the paper (see Eq. (2)), the control input, u_c, depends on the forces transmitted to the support (Eq. (5a)). In a practical implementation, the forces transmitted to the support (calculated in the present paper for specified F_0) would be measured, and the input, u_c, determined based on these measurements. Thus, neither the amplitude nor the phase of the disturbance needs to be known. Although the disturbance frequency, Ω, is specified in the present study, a Fourier analysis of the measured support force, F_s, would readily yield this frequency. Thus, it should be emphasized that the semi-active control methodology developed in the present paper could be applied for any disturbance rejection or vibration isolation problem where the disturbance is harmonic. Beyond that, no information on the disturbance frequency, amplitude, or phase, is really necessary.

A frequency-to-time domain conversion (F/T) unit is used to obtain the time-domain input, u, corresponding to the frequency-domain input, u_c, calculated in Eq. (5) (see Fig. 2). The amplitude of the time-domain input is also calculated during the conversion, and the input is modified if necessary to ensure that maximum or minimum values of physically achievable damping coefficient are not exceeded. This is discussed in greater detail in the next section.

3.2.2. Controllable damper saturation consideration

In the present study the semi-active controllable damper has a baseline damping coefficient of C_0, and it is assumed that the maximum and minimum physically achievable values of damping are $C_0 + C_1$ and $C_0 - C_1$, respectively. Typically C_1 would be some fraction of C_0, and is assumed to be $0.75C_0$ in the present study (following test data of a controllable damper from Ref. [35]). It can be deduced from Eq. (1) that the range of variation in u is

$$-1 \leqslant u \leqslant 1. \tag{6}$$

If the actual dimensional input voltage required for a maximum possible increase of C_1 in damping is u_0 volts (and the corresponding voltage for a maximum possible reduction is $-u_0$

volts), then u effectively represents a non-dimensional voltage input (non-dimensionalized by u_0). In the F/T conversion unit (Fig. 2), the input in the time domain, $\hat{u}(t)$, is examined and if its maximum value, u_{max}, exceeds the maximum permissible value (of unity), then the time domain input signal, $\hat{u}(t)$, can be "scaled down" as follows:

$$u(t) = \frac{\hat{u}(t)}{u_{max}}. \tag{7}$$

Alternately, the input can be reduced by increasing the input penalty weight, W_2.

3.2.3. Frequency content of the semi-active input, u_c

In order to reject a tonal disturbance of frequency, Ω, a semi-active input at twice the disturbance frequency is introduced. This is very different from a fully active system where the control input, u_c, would simply consist of cosine and sine components at the disturbance frequency, Ω, to cancel the support vibrations, z, at Ω. For the system under consideration, the bi-linear semi-active force $C_1 u\dot{x}$ is essentially being used to cancel, as best as possible, the $C_0\dot{x} + Kx$ contribution at the support (see Eq. (2b) and Fig. 1). A semi-active control input at Ω (producing damping variation, $C_1 u$, at Ω), would result in a semi-active force $C_1 u\dot{x}$ at frequency 2Ω, due to the bi-linear $u\dot{x}$ term. Thus, there would be no rejection of the disturbance at Ω, and additionally support vibrations would now be introduced at 2Ω. Instead, a semi-active input (damping modulation) at 2Ω would directly result in forces (proportional to $u\dot{x}$) at Ω and 3Ω, with the component at Ω then canceling the incoming disturbance. Thus, for the present problem the semi-active input, u_c, and output, z (used in minimization of objective function, J, Eq. (3)), are selected as

$$u_c = [u^{2\Omega c} \quad u^{2\Omega s}]^{\mathrm{T}}, \quad z = [F_s^{\Omega c} \quad F_s^{\Omega s}]^{\mathrm{T}}. \tag{8a, b}$$

In the above equations, the superscripts "c" and "s" represents cosine and sine components, respectively, at the corresponding frequencies (Ω or 2Ω). It should be noted that while the selected input, $u = u^{2\Omega c}\cos 2\Omega t + u^{2\Omega s}\sin 2\Omega t$, will reduce the incoming disturbance at Ω, the support will now inevitably experience additional forces at 3Ω. The additional forces could, in principle, be attenuated by expanding z to include the higher harmonic components, and introducing additional harmonics in the input u_c, as well.

Even though semi-active control will produce some higher harmonic vibratory forces (active control will not), the power requirements are expected to be relatively small compared to an isolation strategy using pure active control. In some cases small-to-moderate levels of forces transmitted at higher harmonics may be acceptable, especially when the support itself is a dynamic system—for example, a helicopter with the rotor as the vibratory source and the hub or the fuselage as the support. The forces transmitted at higher harmonics may avoid resonances in the fuselage, and viscoelastic damping treatments are usually more effective at higher frequencies.

3.2.4. Identification of the transfer matrix, T

The system transfer matrix, T, can be identified using both off-line and on-line approaches. Off-line identification of the T matrix is achieved by perturbation of individual components of the input vector, u_c. The first column of T matrix, which corresponds to the first input of u_c (denoted as u_c^1), is obtained by setting $u_c^1 = u^{2\Omega c}$ to a non-zero value (while the other inputs are set to zero),

and the column is then calculated as

$$\begin{bmatrix} t_{11} \\ \vdots \\ t_{1n} \end{bmatrix} = \frac{z - z_0}{u_c^1}. \tag{9}$$

This process is repeated for all entries of the input vector, u_c, to obtain all the columns of the T matrix.

For the on-line identification of the T matrix, an initial estimate is obtained using the batch least-squares method [36], and it is updated using the recursive least-squares method (with variable forgetting factors) [37]. The on-line batch least-square methods yields an initial estimate of the T matrix from an array of inputs, u_c, and corresponding support vibration measurements, z, at $m+1$ time steps, as follows:

$$T = Z\Phi^{\mathrm{T}}(\Phi\Phi^{\mathrm{T}})^{-1}, \quad \Phi = [u_c(k) \quad u_c(k-1) \quad \cdots \quad u_c(k-m)],$$
$$Z = [z(k) \quad z(k-1) \quad \cdots \quad z(k-m)], \tag{10a–c}$$

where $u_c(k)$ and $z(k)$ represents the input and the corresponding support vibration level at the kth time step. It should be noted that the number of time steps used has to be greater than or equal to the number of inputs. For the simulations in the present study, a value of $m = 4$ was used. For the batch least squares, an interval of six disturbance cycles was used between the successive inputs.

An on-line recursive least-squares method is implemented for introducing updates to the T matrix. A variable forgetting factor, λ, is used to prevent parameter estimation 'blow-up', which can occur when the estimation is running continuously for a long time without any change in the parameters being estimated. The recursive least-squares identification is summarized as follows:

$$T(k) = T(k-1) + \varepsilon(k)K(k), \quad \varepsilon(k) = z(k) - T(k-1)u_c(k), \tag{11a, b}$$

$$K(k) = [I + u_c^{\mathrm{T}}(k)P(k-1)u_c(k)]^{-1}u_c^{\mathrm{T}}(k)P(k-1),$$
$$P(k) = \frac{P(k-1)}{\lambda(k)}[I - u_c(k)K(k)], \tag{11c, d}$$

$$\lambda(k) = 1 - [1 - K(k)u_c(k)]\frac{\varepsilon^{\mathrm{T}}(k)\varepsilon(k)}{\Sigma_0}, \tag{11e}$$

where Σ_0 was chosen to be 0.0005, and the lower limit of λ was set at 0.15, in the present study. Updates to $T(k)$ were carried out at intervals of four disturbance cycles.

3.3. Open-loop controller

An open-loop control scheme can in principle be effective for narrowband disturbance rejection (tonal vibration isolation) if the disturbance force and the system are not changing with time. In such a situation, the control input, u_c, is based only on the *baseline* (*uncontrolled*) *support vibration levels*, z_0, as seen in Eq. (5), (and not on any measurements of "current" vibration levels). Once the uncontrolled support vibration, z_0, is determined, and the transfer matrix, T, is obtained using the off-line identification, the open-loop control scheme can be implemented following a block diagram shown in Fig. 3.

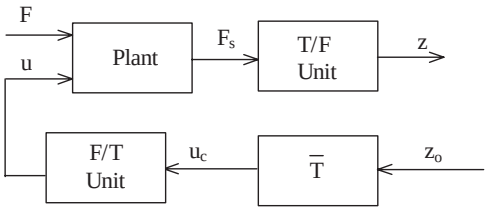

Fig. 3. Block diagram of open-loop control system.

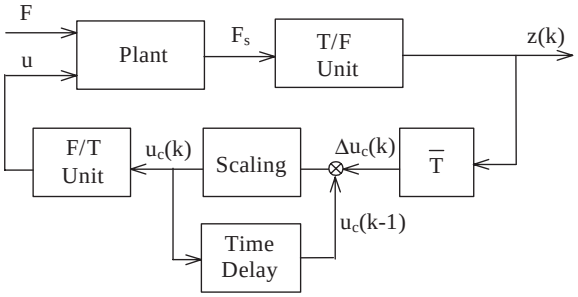

Fig. 4. Block diagram of closed-loop control system.

3.4. Closed-loop controller

If the disturbance force changes during the course of operation, an open-loop algorithm is in general no longer suitable and a closed-loop algorithm has to be employed instead. Using an approach adapted from Ref. [38], previously applied to the active vibration reduction problem, the closed-loop control scheme for the present semi-active disturbance-rejection problem is implemented in the discrete-time domain. The idea is to calculate adjustments in input, Δu_c, based on "current" support vibration levels, $z(k)$, such that vibration levels in the next time step are minimized. In such a case,

$$\Delta u_c(k) = \bar{T} z(k) \tag{12}$$

with $\bar{T}$ identical to that in Eq. (5), and the T matrix identified off-line, a priori. The total input to the controllable damper is then expressed as

$$u_c(k) = u_c(k-1) + \Delta u_c(k). \tag{13}$$

The block diagram corresponding to such a closed-loop control scheme is shown in Fig. 4. Updates to the inputs, $\Delta u_c(k)$, are carried out at intervals of every two disturbance cycles, based on (calculated or measured) support vibration levels, $z(k)$, at these times.

3.5. Closed-loop adaptive controller

In addition to basing control inputs on currently measured vibration levels to allow for variations in disturbance force, the system transfer matrix, T, would require identification and updating on-line if the system is undergoing changes (making it a closed-loop adaptive control scheme). However, the present semi-active system is non-linear (bi-linear), and the results in

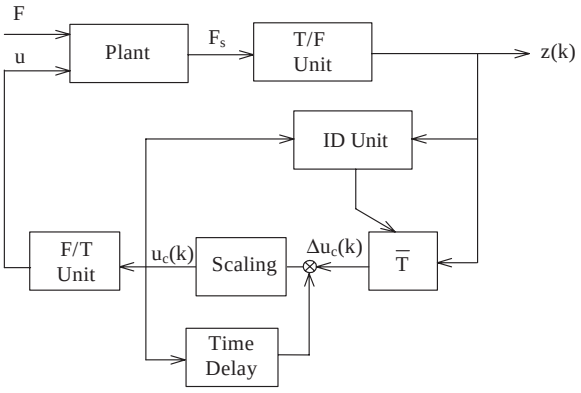

Fig. 5. Block diagram of closed-loop adaptive control system.

Sections 4.3 and 4.4 will show that on-line identification of the transfer matrix is required for effective disturbance rejection even when the system properties are not changing (and only the input disturbance changes) during operation. A detailed explanation of this phenomenon is provided in Section 4.4. The closed-loop adaptive control algorithm is simply the closed-loop scheme described in the previous section with the controller gain, $\bar{T}$ (in Eqs. (5) and (12)), updated using on-line identification of the transfer matrix, T (as described earlier in Section 3.2.4). The block diagram for this closed-loop adaptive controller is shown in Fig. 5.

4. Results and discussion

4.1. Baseline system

Numerical simulations are carried out to evaluate the effectiveness of semi-active control (modulation in damping coefficient of the controllable damper) in rejecting the forces transmitted to the support due to harmonic disturbance inputs. The system parameters used in the simulations are given in Table 1. The baseline support force, F_s (z_0 in the frequency domain), due to a disturbance force, $F_0 \sin(\Omega t)$, is first calculated in the absence of any variations in damping (see Fig. 6). From Fig. 6(b), the amplitude of the support force is seen to be 41% of the disturbance force, this attenuation being due to the passive isolation characteristics of C_0 and K in parallel. It should be noted that for the parameters in Table 1 ($\omega_n = 1$ rad/s, $\Omega = 2$ rad/s—greater than the crossover frequency), the baseline system is operating in the isolation range, and has good passive isolation characteristics. In the following simulations, further reductions in the transmitted vibratory forces due to semi-active modulation of damping coefficient are compared to this baseline vibration level (due to pure passive isolation).

4.2. Open-loop control scheme

In this section, additional reductions in the disturbance transmitted to the support are examined when an open-loop control scheme is used. The inputs are calculated using Eq. (5), which specifies

Table 1
Numerical values of system parameters

Parameter	Numerical value
m	1 (kg)
K	1 (kg/s^2)
C_0/m	0.4 (1/s)
C_1/C_0	0.75
F_0/m	1 (N/kg)
Ω	2 rad/s

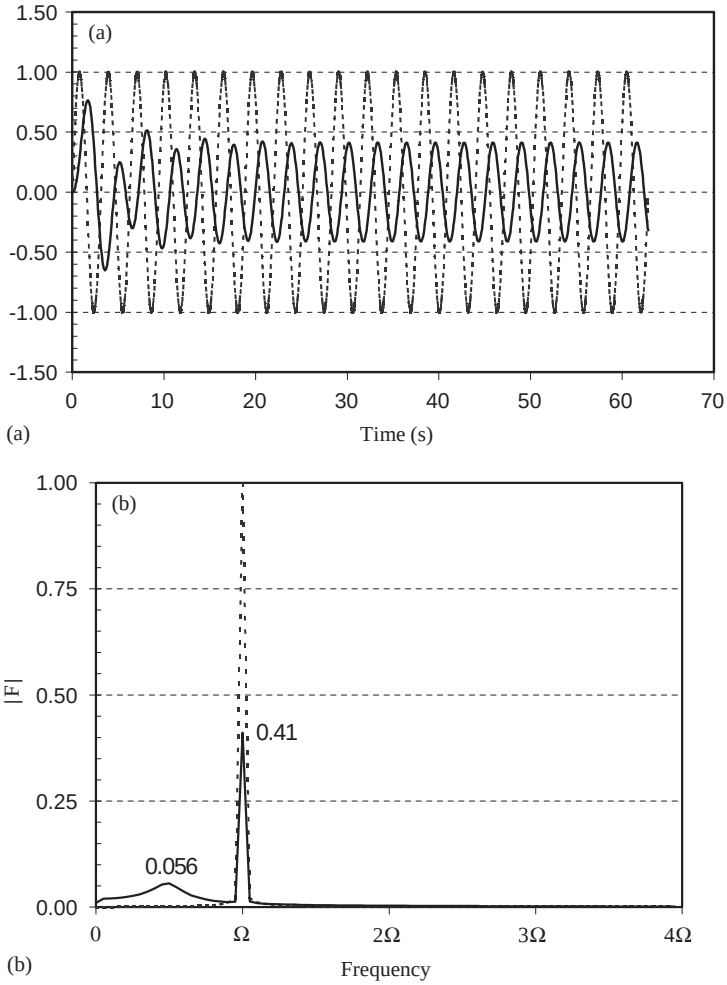

Fig. 6. (a) Time history, and (b) corresponding frequency spectrum of disturbance force, F (dashed line), and support force, F_s (solid line), for the baseline uncontrolled system.

the damping modulation required to minimize the support vibration at frequency Ω. The first set of simulations used a penalty weighting of $W_1 = I$ (identity matrix), and $W_2 = 0$. Further, no "scaling down" of the control inputs was carried out (as described in Section 3.2.2). For the control inputs determined directly from Eq. (5), $u^{2\Omega c} = -2.4527$ and $u^{2\Omega s} = -2.1057$, Fig. 7 shows the frequency content of the steady state vibratory forces transmitted to the support. Although the amplitude of the support force at the disturbance frequency, Ω, is seen to be reduced to 9% of the excitation force amplitude (compared to a force transmissibility of 41% in the absence of any damping modulations), a higher harmonic component at 3Ω (with an amplitude of 26% of the disturbance force) is now observed. This, of course, is expected due to the $C_1\dot{x}u$ term as discussed in Section 3.2.3. From this perspective, some of the disturbance energy can effectively be thought of as being transferred to higher harmonics. This may be advantageous in certain conditions when it is important to avoid specific frequencies due to resonances (e.g., when the harmonic forces from an engine, propeller or helicopter rotor are transmitted to the fuselage), or to exploit the improved effectiveness of viscous and viscoelastic damping mechanisms at higher frequencies. However, it should be noted that the amplitude of the control input, $|u| = |u^{2\Omega}| = \sqrt{(u^{2\Omega c})^2 + (u^{2\Omega s})^2}$, exceeds unity, so the condition on the maximum permissible input, specified in Eq. (6), is violated. For the system considered, it is clear that the control input, or damping variation, that would minimize the transmitted support force is not practically realizable. When the damping variations required exceed the limits of the controllable damper, energy input into the system would actually be required to achieve the levels of disturbance rejection at Ω seen in Fig. 7, and the system would no longer be semi-active.

In the next set of simulations, the control inputs were "scaled down" (as described in Section 3.2.2), so that the inputs ($u^{2\Omega c} = -0.7613$ and $u^{2\Omega s} = -0.6487$) never exceeded the maximum permissible values. In this case, Fig. 8 shows that the amplitude of the transmitted force at the disturbance frequency, Ω, is 29% of the disturbance force amplitude. Compared to a corresponding value of 41% in the absence of damping variation (recall Fig. 6(b)), this represents an additional 32% reduction in transmitted vibration over that achieved due to the pure passive

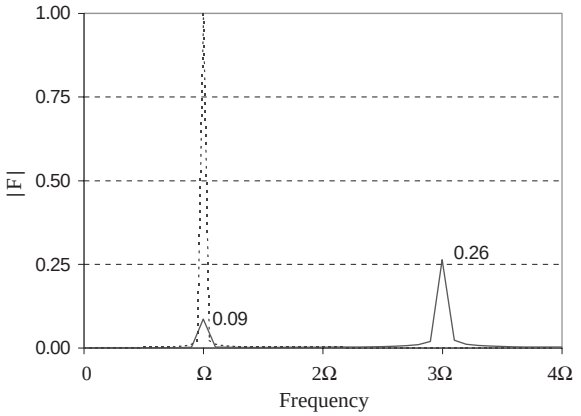

Fig. 7. Frequency spectrum of disturbance force, F (dashed line), and support force, F_s (solid line), due to "optimal" semi-active control input (no input limits).

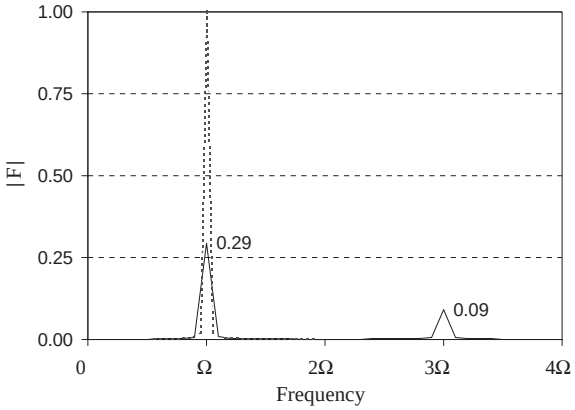

Fig. 8. Frequency spectrum of disturbance force, F (dashed line), and support force, F_s (solid line), due to semi-active control with input "scaled-down" to avoid saturation.

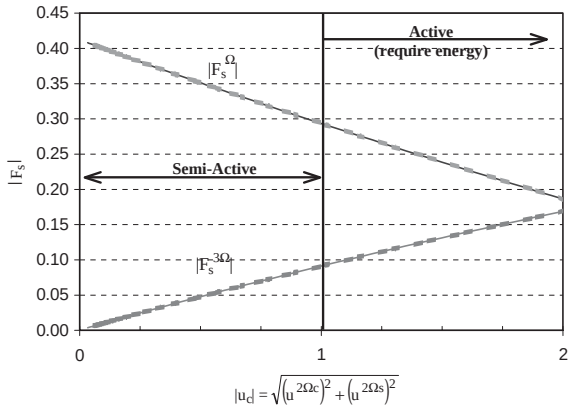

Fig. 9. Variation in the magnitude of the Ω and the 3Ω components of the support force, F_s, as a function of control input amplitude (dashed line—increasing W_k, solid line—scaling).

isolation characteristics. The amplitude of the higher harmonic component at 3Ω is now 9% of the disturbance force amplitude.

Fig. 9 shows the force magnitude of the force transmitted to the support (both at the disturbance frequency, Ω, as well as the higher harmonic component at 3Ω), corresponding to different amplitudes of control input, u_c. Vibration levels corresponding to control inputs greater than unity represent only a mathematical solution not practically achievable by the controllable damper considered. In fact, for $|u_c| > 1.33$, the total damping coefficient would actually be *negative* over parts of the cycle. Since energy input would be required to realize the solutions corresponding to $|u_c| \geqslant 1$, this region has been marked as "active" in Fig. 9. Examining the vibratory support forces corresponding to different "semi-active" inputs, it can be observed that as the control input increases, the support force at the disturbance frequency decreases linearly (producing up to an additional 32% reduction over the passive isolation case for the present

system), and the 3Ω component increases linearly. The control input levels were varied using two different methods—(1) the "scaling down" approach; and (2) using different values of the input penalty weighting, W_2; and the transmitted support forces were found to be identical. Since scaling-down is simple and convenient, it is used in all subsequent simulations.

4.3. Closed-loop control scheme

Benefits to using a closed-loop controller are expected when the disturbance changes during operation. In this section, the performance of both open-loop as well as closed-loop controllers are examined *when the disturbance phase changes during the simulation*. For the closed-loop controller, the control inputs are updated based on Eqs. (12) and (13) at intervals of every two disturbance cycles. The change in disturbance phase, ϕ, is introduced at $t = 10\pi$ s, as described below:

$$F(t) = \begin{cases} F_0 \sin(\Omega t), & 0 \leqslant t < 10\pi, \\ F_0 \sin(\Omega t + \phi), & t \geqslant 10\pi. \end{cases} \tag{14}$$

For a phase change of $\phi = 45^\circ$, Fig. 10 shows the time history of the disturbance, as well as the force transmitted to the support, when the closed-loop controller is operational. It is seen that even after the change in disturbance phase occurs, the closed-loop controller is once again able to reduce the support vibration levels, in a short duration. Fig. 11 shows the amplitude of the support force at the disturbance frequency, Ω, using both open- and closed-loop controllers. As expected, the open-loop controller is no longer effective in disturbance rejection after the disturbance phase changes (since the control inputs, which are based only on the initial support forces, are no longer effective after the disturbance phase, and therefore the phase of the current support forces changes). However, with the closed-loop controller, after a transition period, the disturbance transmitted to the support is once again reduced. When a disturbance phase change of $\phi = 90^\circ$ is introduced, Fig. 12 once again shows that the closed-loop controller performs better than the open-loop controller. For the 45° change in phase angle, the closed-loop control inputs

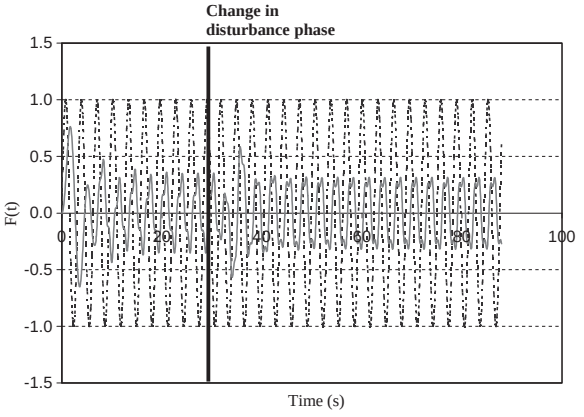

Fig. 10. Time history of disturbance force, F (dashed line), with a change in phase of 45°, and support force, F_s (solid line), using closed-loop semi-active control.

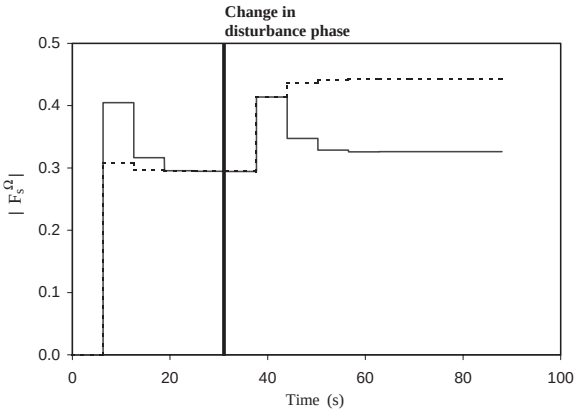

Fig. 11. Amplitude of support force, F_s, at disturbance frequency, Ω, for open-loop (dashed line) and closed-loop (solid line) control, with a change in disturbance phase of 45°.

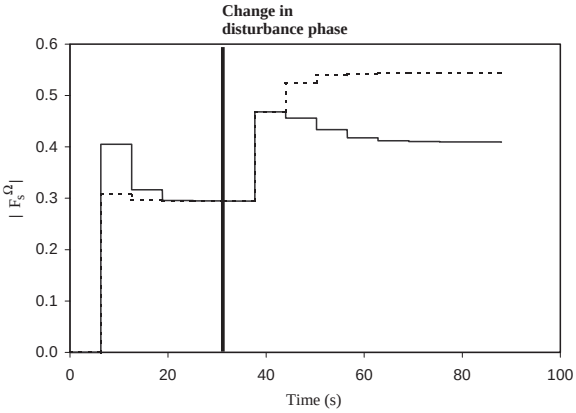

Fig. 12. Amplitude of support force, F_s, at disturbance frequency, Ω, for open-loop (dashed line) and closed-loop (solid line) control, with a change in disturbance phase of 90°.

are changed to $u^{2\Omega c} = -0.958$ and $u^{2\Omega s} = 0.2852$, and the corresponding inputs for the 90° disturbance phase change are $u^{2\Omega c} = 0.911$ and $u^{2\Omega s} = -0.413$. It should be noted that although the closed-loop controller is more effective than the open-loop controller, the steady state disturbance levels transmitted to the support are not as low as those prior to change in disturbance phase (as would have been expected if an active force-generator type actuator had been used).

Fig. 13 shows the magnitude of the forces transmitted to the support at the disturbance frequency, Ω, as a function of disturbance phase change (varying between $-90°$ and 90°). It is observed that as the phase change increases, the effectiveness of the open-loop control scheme is degraded significantly, to the extent that the vibratory forces at the support are larger than the passive isolation case (no semi-active cyclic damping modulations) when the change in disturbance phase exceeds $\pm 40°$. Performance degradation is also observed for the closed-loop

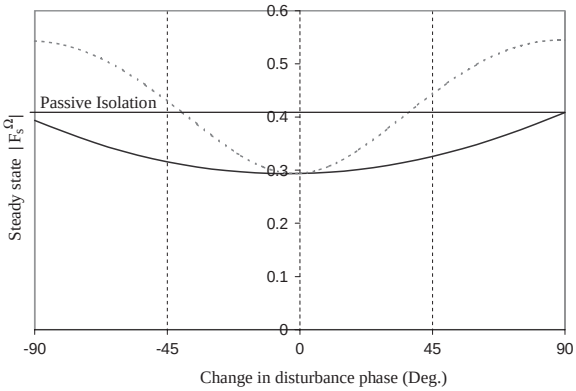

Fig. 13. Amplitude of steady state support force, F_s, at Ω, for open-loop (dashed line) and closed-loop (solid line) controllers, as a function of change in disturbance phase.

scheme, but is milder. The reason that the closed-loop controller is not able to track phase changes perfectly (as would have been expected if an active force-generator type actuator was used) can be explained as follows: for a *pure active controller*, the control force can be generally written as Au (where A is some *constant* coefficient). When the disturbance phase changes by a certain amount during operation, the phase of the response and the vibratory forces transmitted to the support will correspondingly change. The input, u, is then based on the current support forces, and since the active force is simply Au its phase is appropriately adjusted and comparable reductions in support vibrations are obtained. For the *semi-active controller*, however, the control force is $C_1\dot{x}u$. Thus, when the disturbance phase changes, the response (x and $\dot{x}$), support force, and control input, u (proportional to the current support force), would undergo corresponding phase changes, but the change in phase of the bi- semi-active force, $C_1\dot{x}u$, is no longer proportional to the change in disturbance phase (as was the case with pure active control). This suggests that an adaptive controller (recalculating the system transfer matrix, T, online) may be required for the semi-active narrowband disturbance rejection if the disturbance is likely to change during operation, even when the system parameters themselves remain unchanged.

4.4. Closed-loop adaptive control scheme

The effectiveness of the closed-loop adaptive controller is evaluated in this section when the disturbance phase changes during operation. Online identification of the transfer matrix, T, using batch least-squares approach (Eq. (10)) for initial estimates and recursive least-squares identification (Eq. (11)), for updates is carried out, as described in Section 3.2.4. For the present simulations, updates of the transfer matrix (in the recursive least-squares approach) were carried out every four disturbance cycles. The disturbance phase changes as described in Eq. (14), except that it is introduced at $t = 32\pi$ s (instead of 10π s). The first 24π s is used for batch least-squares identification of the T matrix by inputting a sequence of small input signals, at the end of which period the controller is switched on. Figs. 14 and 15, respectively, show the variation of the support force amplitude at the disturbance frequency, Ω, for disturbance phase changes of 45°

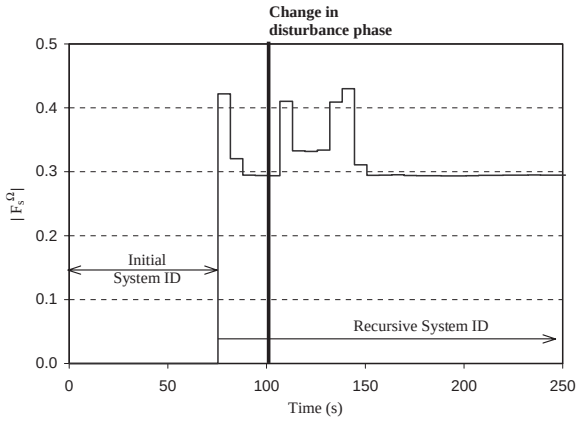

Fig. 14. Amplitude of support force, F_s, at disturbance frequency, Ω, for closed-loop adaptive control, with a change in disturbance phase of 45°.

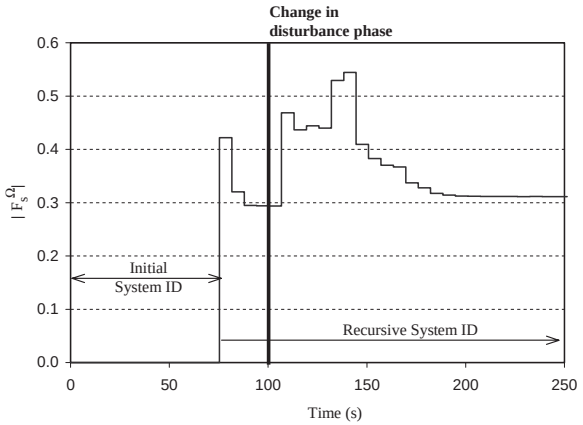

Fig. 15. Amplitude of support force, F_s, at disturbance frequency, Ω, for closed-loop adaptive control, with a change in disturbance phase of 90°.

and 90°. It is seen from both figures that when the adaptive controller is operational, after a transition period, the support vibratory forces are reduced to levels prior to the change in disturbance phase (unlike the "non-adaptive" closed-loop controller that did not retain its effectiveness; recall Figs. 11–13).

Fig. 16 shows the steady state support vibrations at the disturbance frequency, Ω, as a function of disturbance phase change (varying between $-90°$ and 90°). It is observed that even as there is an increase in disturbance phase change, unlike the open- and closed-loop controllers, the closed-loop adaptive controller completely retains its effectiveness in reducing support vibrations. Thus, for a semi-active (bi-linear) system, a closed-loop adaptive controller (continuous on-line identification of system transfer matrix) is required even when there is only a disturbance change, and not a "direct" change in system properties. Although, it could be said that for a non-linear

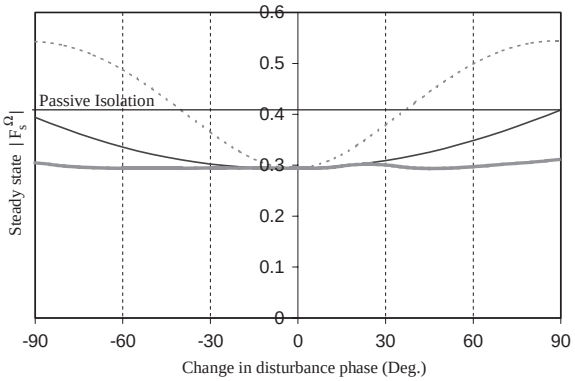

Fig. 16. Amplitude of steady state support force, F_s, at Ω, for open-loop (dashed line), closed-loop (solid line), and closed-loop adaptive (thick line) controllers, as a function of change in disturbance phase.

semi-active system, the ''system'', as such, is dependent on the excitation, so a change in the disturbance changes the system itself.

4.5. *Effectiveness of cyclic damping modulation with variation in baseline damper size*

Results in Sections 4.2–4.4 have indicated that modulating the damping coefficient at twice the disturbance frequency, Ω, can produce additional reductions in the transmitted disturbance (at Ω) of the order of around 30%; beyond the reductions observed due to the passive isolation characteristics. Of course, the passive isolation characteristics, themselves, strongly depend on the baseline damping (and stiffness) in the system. This section examines how the effectiveness of cyclic modulation of damping coefficient in further reducing transmitted disturbance changes if the baseline damping of the system (the basic damper size) is changed. This implies a change in the value of C_0, relative to the other system parameters, K and m. However, the maximum value of C_1 is held at $0.75C_0$, so that even as the damper is scaled up or down its basic characteristics are unchanged and the variation in damping available, relative to the baseline, remains at 75%. For the baseline system parameters used in Table 1, the passive damping ratio of the SDOF system in Fig. 1 (Eq. 2(a)) is 20%. When this value of damping ratio is varied (through variation in the value of C_0), the corresponding change in support vibration level (at disturbance frequency, Ω) is shown in Fig. 17. As expected, the passive isolation characteristics are not as good for increasing values of damping ratio (increasing C_0), and vice versa. The effectiveness of cyclic modulation of damping coefficient in further attenuating support vibrations is also shown in Fig. 17. From the figure, semi-active control (cyclic damping modulation at 2Ω) produces maximum additional reductions in support vibrations when the baseline passive damping ratio is around 15–20%, and the benefits decrease for smaller or larger values of baseline passive damping, C_0. It should be noted that with cyclic modulation in damping coefficient the transmitted vibratory forces at the disturbance frequency are lower than the forces transmitted by simply reducing the baseline damping levels, or even setting them to zero (theoretically the best for minimizing transmitted vibratory forces in a passive isolation treatment). It may not always be possible or desirable to reduce the transmissibility by simply minimizing the baseline damping (since resonant responses

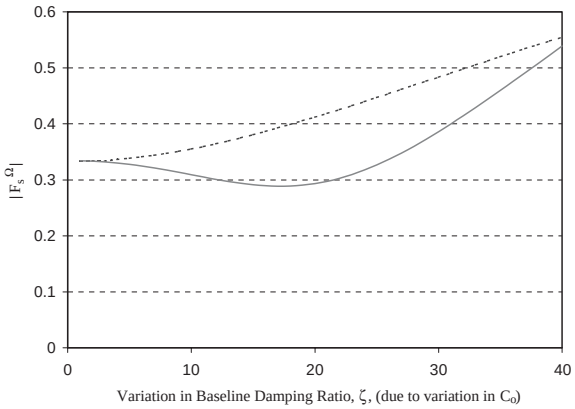

Fig. 17. Amplitude of support force, F_s, at Ω, (transmissibility) as a function of baseline damping, for passive isolation (dashed line) and semi-active isolation (solid line).

during spin-up or -down could be very high, and the decay time for transients due to perturbations could be inordinately long). Similarly, reduction of transmissibility by using arbitrarily soft isolation mounts (decreasing K) may not be practical as they could result in large static deformations and large amplitude oscillations of the mass, m, when the support is excessively compliant. In such cases, cyclic modulation of the damping coefficient for additional reductions in transmissibility may be particularly attractive.

5. Summary and concluding remarks

The present study examines the potential of using a semi-active controllable damper, whose damping coefficient can be modulated in real time, for narrowband disturbance rejection (tonal vibration isolation) applications. For a harmonic disturbance, a control algorithm is developed in the frequency domain for determining the input (cyclic damping modulation) that minimizes the force transmitted to the support at the disturbance frequency. An input, u, with a frequency of twice the disturbance frequency is used, so that the resulting bilinear semi-active force (proportional to $\dot{x}u$) has a component at the disturbance frequency that cancels the force at the support. Such a scheme, however, will inevitably result in some higher-harmonic support force. The effectiveness of open-loop, closed-loop, and adaptive controllers in rejecting the transmitted forces at the disturbance frequency are evaluated. Some of the key observations of the present study are presented next.

When the calculated variations in damping exceeded the specified limits, input scaling was used, and the magnitude of the support force at the disturbance frequency could be reduced by about an additional 30%, beyond the levels due to the passive isolation characteristics (no cyclic damping modulation). When the disturbance phase changed during operation, the performance of the open-loop controller rapidly degraded, as the inputs based on the initial ($t = 0$) support forces were no longer correctly phased. While the closed-loop controller performed somewhat better (and generally reduced support vibratory forces to levels lower than those due to pure passive

isolation), there was still some performance degradation; and support forces could not be reduced to levels prior to change in disturbance phase, as would have been expected in the case of closed-loop control using an active force-generator type actuator. However, when a closed-loop adaptive controller was used (with on-line system identification), the reduction in transmitted support force was completely maintained even after the disturbance phase underwent change. Thus it is seen that for narrowband disturbance rejection using a semi-active system (which is bi-linear), a closed-loop adaptive control scheme is required if the disturbance is likely to change during operation, even if the basic system parameters themselves are unchanged. Results showed that cyclic modulations in the damping coefficient were more effective in reducing the transmitted forces at the disturbance frequency than simply reducing the baseline damping coefficient (to improve the passive isolation characteristics).

References

[1] G. Reichert, Helicopter vibration control—survey, *Vertica* 5 (1) (1981) 1–20.
[2] R.G. Lowey, Helicopter vibrations: a technological perspective, *Journal of the American Helicopter Society* 29 (4) (1984) 4–30.
[3] C.M. Harris, *Shock and Vibration Handbook*, McGraw-Hill, New York, 1988.
[4] A.E. Staple, An evaluation of active control of structural response as a means of reducing helicopter vibration, *Proceedings of the 15th European Rotorcraft Forum*, Amsterdam, Netherlands, September 1989, pp. 51.1–51.18.
[5] S.S. Rao, *Mechanical Vibrations*, Addison-Wesley, Reading, MA, 1990.
[6] K.B. Scribner, L.A. Sievers, A.H. von Flotow, Active narrow-band vibration isolation of machinery noise from resonant substructures, *Journal of Sound and Vibration* 167 (1) (1993) 17–40.
[7] M.D. Jerkins, R.J. Nelson, R.J. Pinnington, S.J. Elliott, Active isolation of periodic machinery vibrations, *Journal of Sound and Vibration* 166 (1) (1993) 117–140.
[8] D.J. Inman, *Engineering Vibration*, Prentice-Hall, Englewood Cliffs, NJ, 1994.
[9] W. Welsh, C. Fredrickson, C. Rauch, I. Lyndon, Flight test of an active vibration control system on the UH-60 black hawk helicopter, *Proceedings of the American Helicopter Society 51st Annual Forum*, May 1995, pp. 393–402.
[10] J.Q. Sun, M.R. Jolly, M.A. Norris, Passive, adaptive and active tuned vibration absorbers—a survey, *Journal of Mechanical Design, Transactions of the American Society of Mechanical Engineers* 117 B (1995) 234–242.
[11] R.L. Williams II, Survey of active truss modules, *American Society of Mechanical Engineers, Design Engineering Division* 82 (1) (1995) 899–906.
[12] J.N. Yang, J.C. Wu, Z. Li, Control of seismic-excited buildings using active variable stiffness systems, *Engineering Structures* 19 (9) (1996) 589–596.
[13] W.N. Patten, C. Mo, J. Kuehn, J. Lee, A primer on design of semiactive vibration absorbers (SAVA), *Journal of Engineering Mechanics* 124 (1) (1998) 61–68.
[14] F. Sadek, B. Mohraz, Semiactive control algorithms for structures with variable dampers, *Journal of Engineering Mechanics* 124 (9) (1998) 981–990.
[15] H.P. Gavin, N.S. Doke, Resonance suppression through variable stiffness and damping mechanisms, *Proceedings of the SPIE Smart Structures Conference*, SPIE, Vol. 3671, March 1999, pp. 43–53.
[16] E.J. Krasnicki, Comparison of analytical and experimental results for a semi-active vibration isolator, *The Shock and Vibration Bulletin*, Vol. 50 (4), The Shock and Vibration Information Center, Naval Research Laboratory, Washington, DC, 1980 pp. 69–76.
[17] E.J. Krasnicki, The experimental performance of an off-road vehicle utilizing a semi-active suspension, *The Shock and Vibration Bulletin*, Vol. 54 (3), The Shock and Vibration Information Center, Naval Research Laboratory, Washington, DC, 1984 pp. 135–142.
[18] D. Hrovat, D.L. Margolis, M. Hubbard, An approach toward the optimal semi-active suspension, *Journal of Dynamic Systems, Measurement and Control* 110 (1988) 288–296.

[19] D. Karnopp, Design principles for vibration control using semi-active dampers, *Journal of Dynamic Systems, Measurement and Control* 112 (1990) 448–455.
[20] G.M. Kamath, N.M. Wereley, M.R. Jolly, Characterization of magnetorheological helicopter lag dampers, *Journal of the American Helicopter Society* 44 (3) (1999) 234–248.
[21] Y.S. Zhao, Y.T. Choi, N.M. Wereley, Semi-active damping of ground resonance in helicopters using magnetorheological dampers, *Proceedings of the 57th Annual Forum of the American Helicopter Society*, Washington DC, May 2001.
[22] S. Marathe, F. Gandhi, K.W. Wang, Helicopter blade response and aeromechanical stability with a magnetorheological fluid based lag damper, *Journal of Intelligent Material Systems and Structures* 9 (4) (1998) 272–282.
[23] P. Anusonti-Inthra, F. Gandhi, L. Miller, Reduction of helicopter vibration through cyclic control of variable orifice dampers, *The Aeronautical Journal*, The Royal Aeronautical Society, 2003, in press.
[24] M.D. Symans, M.C. Constantinou, Semi-active control system for seismic protection of structures: a state-of-the-art review, *Engineering Structures* 21 (1999) 469–487.
[25] A. Hac', I. Youn, Optimal semi-active suspension with preview based on a quarter car model, *Journal of Vibration and Acoustics* 114 (1992) 84–92.
[26] K. Yi, M. Wargelin, K. Hedrick, Dynamic tire force control by semi-active suspensions, *American Society of Mechanical Engineers, Dynamic Systems and Control Division* 44 (1992) 299–310.
[27] M.D. Symans, M.C. Constantinou, Seismic testing of a building structure with a semi-active fluid damper control system, *Earthquake Engineering and Structural Dynamics* 26 (1997) 759–777.
[28] S.J. Dyke, B.F. Spencer Jr., M.K. Sain, J.D. Carlson, An experimental study of MR dampers for seismic protection, *Smart Materials and Structures* 7 (5) (1998) 693–703.
[29] J. Onoda, T. Endo, H. Tamaoki, N. Watanabe, Vibration suppression by variable-stiffness members, *American Institute of Aeronautics and Astronautics Journal* 29 (6) (1991) 977–983.
[30] M. Fodor, R.C. Redfield, Resistance Control, Semi-active damping performance, *American Society of Mechanical Engineers Advanced Automotive Technology* 56/86 (1995) 161–169.
[31] N.H. McClamroch, H.P. Gavin, Closed loop structural control using electrorheological dampers, *Proceedings of the American Control Conference*, June 1995, pp. 4173–4177.
[32] K. Kawashima, S. Unjoh, Seismic response control of bridges by variable dampers, *Journal of Structural Engineering* 120 (9) (1994) 2583–2601.
[33] M.D. Symans, S.W. Kelly, Fuzzy logic control of bridge structures using intelligent semi-active seismic isolation systems, *Earthquake Engineering and Structural Dynamics* 28 (1999) 37–60.
[34] W. Johnson, Self-tuning regulators for multicyclic control of helicopter vibration, NASA Technical Paper 1996, March 1982.
[35] M.D. Symans, M.C. Constantinou, D.P. Taylor, K.D. Garnjost, Semi-active fluid viscous dampers for seismic response control, *Proceedings of the First World Conference on Structural Control*, 3–5 August 1994, Los Angeles, CA.
[36] K.J. Astrom, B. Wittenmark, *Adaptive Control*, 2nd Edition, Addison-Wesley Publishing Company Inc., Reading, MA, 1995.
[37] T.R. Fortescue, L.S. Kershenbaum, B.E. Ydstie, Implementation of self-tuning regulators with variable forgetting factors, *Automatica* 17 (6) (1981) 831–835.
[38] S.R. Hall, N.M. Wereley, Linear control issues in the higher harmonic control of helicopter vibrations, *Proceedings of the American Helicopter Society 45th Annual Forum*, Boston, MA, May 1989.